Article

Ni-Catalyzed Reductive Coupling of Electron-Rich Aryl Iodides with Tertiary Alkyl Halides

Xuan Wang, Guobin Ma, Yu Peng, Chloe E. Pitsch, Brenda J. Moll, Thu D. Ly, Xiaotai Wang, and Hegui Gong

J. Am. Chem. Soc., **Just Accepted Manuscript** • DOI: 10.1021/jacs.8b09473 • Publication Date (Web): 08 Oct 2018

Ni-Catalyzed Reductive Coupling of Electron-Rich Aryl Iodides with Tertiary Alkyl Halides

Xuan Wang,[†] Guobin Ma,[†] Yu Peng,[§] Chloe E. Pitsch,[‡] Brenda J. Moll,[‡] Thu D. Ly,[‡] Xiaotai Wang*[‡¶] and Hegui Gong*[†]

[†]School of Materials Science and Engineering, Center for Supramolecular Chemistry and Catalysis and Department of Chemistry, Shanghai University, 99 Shang-Da Road, Shanghai 200444, China

[‡]Department of Chemistry, University of Colorado Denver, Campus Box 194, P.O. Box 173364, Denver, Colorado 80217-3364, United States

[¶]Institute of Molecular Science, Shanxi University, Taiyuan, Shanxi 030006, China

[§]State Key Laboratory of Applied Organic Chemistry, College of Chemistry and Chemical Engineering, Lanzhou University, Lanzhou 730000, China

Nickel, tert-Alkyl Halides, Aryl iodides, Quaternary carbon

ABSTRACT: This work illustrates the reductive coupling of electron-rich aryl halides with tertiary alkyl halides under Ni-catalyzed cross-electrophile coupling conditions, which offers an efficient protocol for the construction of all carbon quaternary stereogenic centers. The mild and easy-to-operate reaction tolerates a wide range of functional groups. The utility of this method is manifested by the preparation of cyclotryptamine derivatives, wherein successful incorporation of 7-indolyl moieties is of particular interest as numerous naturally-occurring products are composed of these key scaffolds. DFT calculations have been carried out to investigate the proposed radical chain and double oxidative addition pathways, which provide useful mechanistic insights into the part of the reaction that takes place in solution.

1. INTRODUCTION

All-carbon quaternary stereocenters containing *tertiary* alkyl–aryl bonds are widespread in biologically active natural products and pharmaceutical compounds.[1] Electron-rich arenes are particular prevalent in this class of structural motifs. Notable examples include the (+)-asperazine, (-)-viridicatumotxin B, and (-)-mesembrine families (Figure 1).[2] Numerous cross-coupling protocols have been implemented to access such highly congested quaternary carbon centers; nearly without exception, these have relied on the creation of C(sp^3)–C(sp^2) bonds.[3-7] For instance, Biscoe developed a Ni-catalyzed strategy that involves the coupling of a tertiary alkyl–MgX reagent with aryl halides (Scheme 1).[4] The reaction accommodates a wide array of electron-rich and -poor arenes with high retention to isomerization ratios (R:I) of the alkyl moieties, although functional group compatibility and the scope of alkyl substrates may be restricted because alkyl Grignard reagents are utilized. Recently, a photoredox/Ni-catalyzed Suzuki reaction was reported by Molander, which allows effective coupling of tertiary alkyl trifluoroborates with electron-deficient aryl bromides (Scheme 1).[5] Alternatively, the coupling of tertiary alkyl electrophiles with aryl nucleophiles has been advanced.[6–7] As such, Fu reported a Ni-catalyzed Suzuki method wherein aryl-9-BBN decorated with electron-donating or -neutral groups at the *meta*-positions were coupled with a broad range of unactivated tertiary alkyl bromides; low yields were observed for *ortho*- or *para*-substituted arenes.[6] Here we report the use of 3-fluoropyrinde (3-F–Py) as the additive/ligand that allows an efficient coupling of electron-rich aryl halides with tertiary alkyl halides. The present strategy is in line with our recent interest in the creation of arylated carbon quaternary stereogenic centers through cross-electrophile coupling regimes.[8-13]

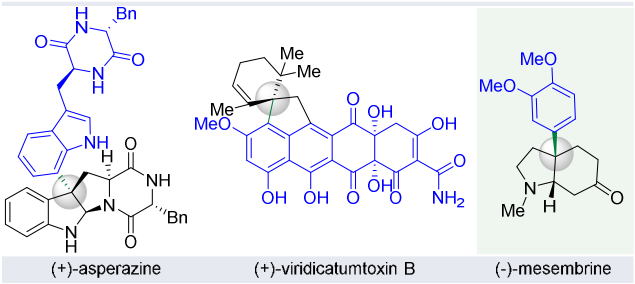

Figure 1. Examples of the bioactive natural products

We have previously shown that the use of Ni/pyridine or 4-dimethylaminopyridine (DMAP) catalytic conditions enables an effective coupling of tertiary bromides with a

diverse set of electron-deficient aryl bromides (Scheme 1).[13] Electron-rich aryl halides are incompetent due to low coupling efficiency and severe isomerization of the alkyl groups. This method thus fell short of addressing the challenge needed to create the key aryl–tertiary alkyl bond present in many natural products, such as those shown in Figure 1. As detailed below, we have now developed a Ni/3-F–Py-catalyzed method that allows direct coupling of tertiary alkyl halides and electron rich iodoarenes. The practicability of our method is illustrated by the facile joining of C3(sp^3) of cyclotryptophan with C8'(sp^2) indole derivatives. This represents a potentially complementary solution to the long-standing bottleneck in the synthesis of (+)-asperazine and its analogs.[2b,14]

Scheme 1. Creation of Quaternary Carbon Centers through Ni-Catalyzed Aryl–Alkyl Bond Formation

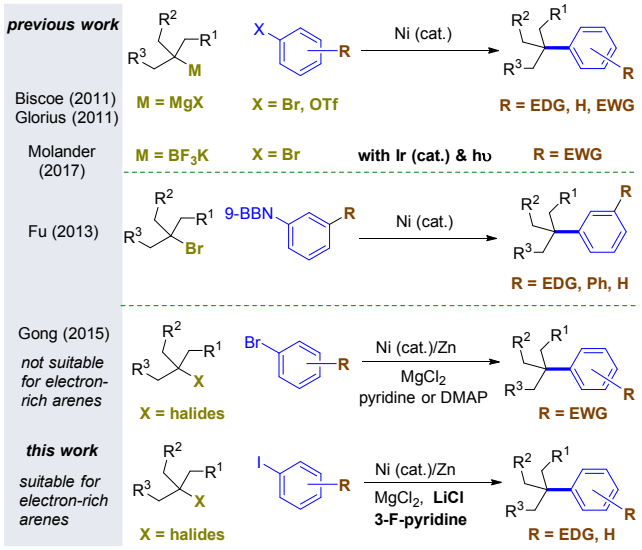

2. RESULTS AND DISSCUSIONS

2.1. Optimization and Substrate Scope

Table 1. Optimization for the Reaction of 1 with 4-iodoanisole [a]

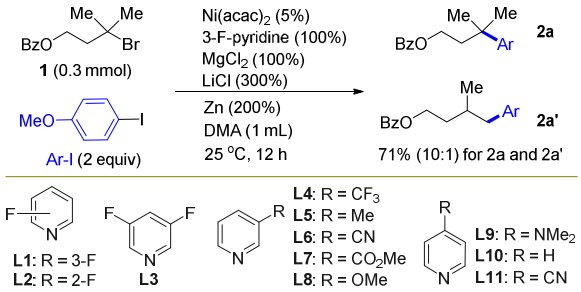

Entry[a]	Variation from the standard conditions	Yield[b]	R:I[c]
1	no changes	65% (71%)[d]	10:1
2	w/o Ni	trace	NA
3	w/o Zn	trace	NA
4	w/o 3-F pyridine	trace	NA
5	w/o $MgCl_2$	18%	50:1
6	w/o LiCl	30%	12:1
7	50% 3-F pyridine	54%	11:1
8	Mn instead	52%	10:1
9	**L2** instead of **L1**	trace	NA
10	**L3** instead of **L1**	44%	10:1
11	**L4** instead of **L1**	58%	10:1
12	**L5** instead of **L1**	46%	10:1
13	**L6** instead of **L1**	50%	>10:1
14	**L7** instead of **L1**	60%	10:1
15	**L8** instead of **L1**	52%	9:1
16	**L9** instead of **L1**	22%	>20:1
17	**L10** instead of **L1**	50%	6:1
18	**L11** instead of **L1**	50%	20:1

[a] Reaction Conditions: tertiary bromide **1** (0.3 mmol, 100 mol %), 4-iodoanisole (200 mol %), $Ni(acac)_2$ (5 mol %), pyridine derivative (100 mol %), Zn (200 mol %), $MgCl_2$ (100 mol %), LiCl (300 mol %), solvent (1 mL). [b] NMR yield using 2,5-dimethylfuran as the internal standard. [c] The ratio of retention to isomerization (R:I) of alkyl groups was determined by ^{1}H NMR analysis of a mixture containing **2a** and **2a'** and other impurities that was obtained after passing the reaction mixture through a short silica column. [d] Isolated yield.

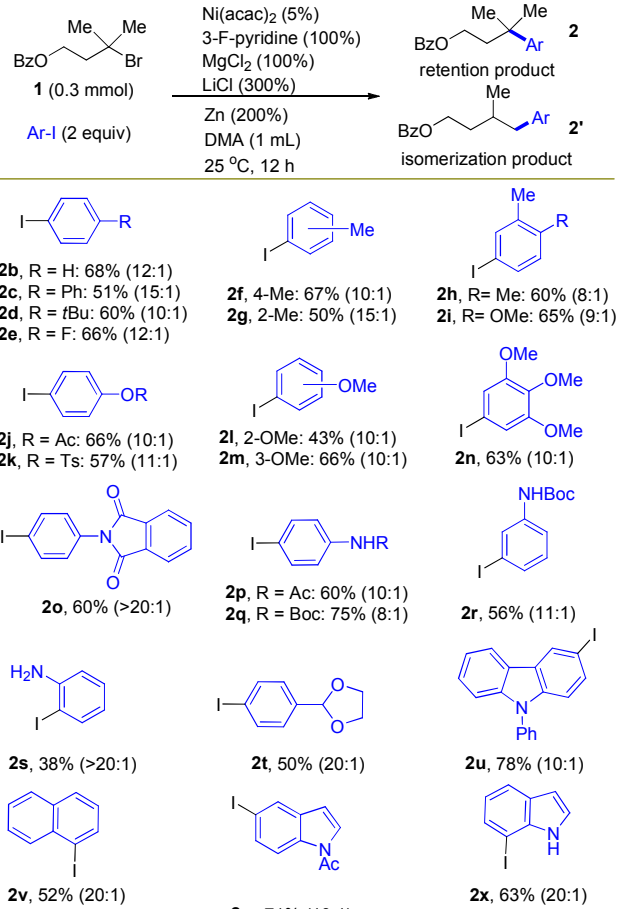

Figure 2. Coupling of **1** with aryl iodides. Reaction conditions are same as in Table 1, entry 1. Isolated yields each refer to a mixture of the quaternary product and its isomer. Shown in parenthesis are ratios of retention to isomerization (R:I) of alkyl groups determined by ^{1}H NMR analysis after purification.

In our previous studies, the coupling of *tertiary* alkyl bromide **1** with 4-bromoanisole using pyridine or DMAP as the additives/ligands gave rise to the cross-coupling product **2a** in less than 5% yield, with most of the 4-bromoanisole remaining intact.[15] To enhance the reactivity of the aryl partner, 4-iodoanisole was chosen, but this

only increased the yield to 8% with a 2:1 ratio of **2a**/**2a'**.[15] Efforts to optimize the reaction conditions were then undertaken (Table 1). It was found that when $Ni(acac)_2$ was used as the Ni(II) source, DMA (dimethylacetamide) as the solvent, and 3-F-pyridine as the putative ligand, a 71% isolated yield was obtained for a mixture of retention product **2a** and its isomer **2a'** in a 10:1 ratio (R:I) in the presence of LiCl, Zn, and $MgCl_2$. Control experiments showed the indispensable role of Ni(II), Zn, and 3-F-pyridine

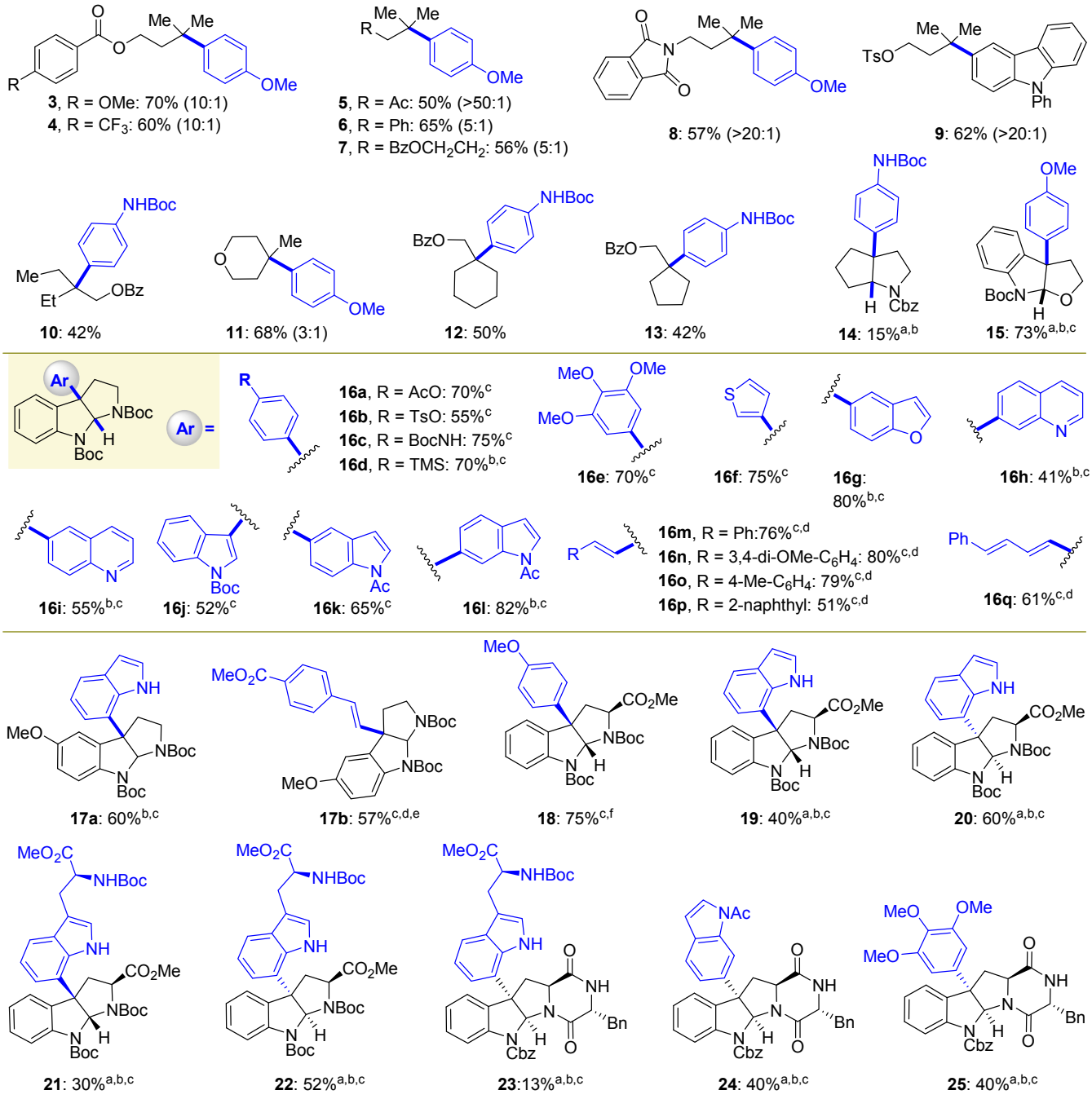

Figure 3. Examination of substrate scope. Unless otherwise indicated the standard reaction conditions same as Table 1, entry 1 were used, and isolated yields for a mixture of the quaternary product and its isomers (if applicable) were obtained. The R:I ratios shown in parenthesis were determined by ^1H NMR after purification. [a] 20 mol % of $Ni(acac)_2$ was used. [b] DMF was used as the solvent. [c] Alkyl chloride was used. [d] The ratio of tertiary alkyl halide to vinyl halide was 1.5:1, and NiI_2 (10 mol %) and DMSO were used. [e] DMAP was used to replace 3-F-pyridine. [f] 5 μL of H_2O was added via a syringe.

(Table 1, entries 2–4). The yields were reduced dramatically in the absence of $MgCl_2$ or LiCl (entries 5–6). Reducing the amount of 3-F–Py also lowered the yield (entry 7). The use of Mn instead of Zn resulted in a comparable isomerization ratio, albeit in a lower overall yield (entry 8). Other pyridine ligands proved less effective (entries 9-18), although the presence of electron-withdrawing groups on the pyridine ring seemed to be beneficial (e.g. **L11** vs **L9**). It should be noted that bipyridine and terpyridine ligands only furnished a trace amount of the coupling products. Monitoring of the reaction revealed that it proceeded to completion within one hour (Figure S15).[16]

Next, a variety of aryl iodides were investigated as coupling partners for **1**.[16] Iodobenzene and its para-substituted derivatives provided the products **2b–2f** in good yields with good control of isomerization ratios (Figure 2). Both *para*- and *ortho*-methyl iodobenzenes were compatible with the reaction conditions, with the former being more effective. Mono-, di- and tri-substituted methyl and/or methoxy aryl iodides generally furnished the coupling products **2g–2n** in good yields and high R:I ratios. However, a moderate result was obtained for 2-methoxy iodobenzene, presumably due to increased steric hindrance. The reaction conditions were also applicable to arenes bearing amino groups. It was found that *meta*- and *para*-substituted acetyl and Boc-protected amino and phthalimidyl groups were coupled effectively, as illustrated by the preparation of **2o–2r**. By contrast, a corresponding substrate bearing a Boc-protected amino group in the *ortho*-position failed to give Boc-protected **2s** in an appreciable yield. 2-Iodoaniline itself gave **2s** in 38% yield with a high R:I ratio. Iodobenzene bearing *para*-acetal furnished **2t** in 50% yield. On other hand, the present coupling approach proved compatible with 3-iodo-9-phenyl-9H-carbazole and 1-iodonaphthalene as evident by the effective preparation of **2u** and **2v**. Finally 5- and 7-iodoindoles were tolerated, with no protecting group proving necessary for the production of **2x**.

The coupling protocol also displayed good compatibility across a range of tertiary alkyl electrophiles.[16] For instance, a variety of 2-bromo-2-methyl alkanes bearing benzoyl esters, ketone, benzyl, and tosylate groups gave products **3–9** in good yields and with good control of R:I ratios. The more sterically hindered 2-bromo-2-ethylbutanol protected with benzoyl furnished **10** in 42% yield without detectable isomerization byproducts. Cyclic alkyl bromides were also examined. 4-Bromotetrahydro-2*H*-pyran resulted in **11** and its isomer in an overall 68% yield with a R:I ratio of 3:1. (1-Bromocyclohexyl)methyl benzoate and its five-membered ring analog gave rise to **12** and **13** in 50% and 42% yields with no detectable isomerization products. Heterocyclic halides are also competent for this quaternary carbon-generating method. A low yield was obtained for **14**, due to a highly competitive dechlorination/decyclization reaction of the tertiary bromide to form Cbz-proteted 2-(cyclopent-1-en-1-yl)ethan-1-amine. Arylation at the benzylic carbon of tetrahydrofuro[2,3]indole resulted in **15** in 73% yield. In both cases of **14** and **15**, the use of 20 mol% of Ni and DMF (instead of DMA) enhanced the coupling yields by inhibiting undesired ring-opening side reactions. This practice is quite general for low yielding arylation of chlorocyclotrypatamine substrates (Figure 3).

To explore further the utility of this coupling strategy, an effort was made to construct cyclotrypatamine analogs.[16] This was done by coupling their chloro-precursors with a number of aryl and vinyl halides. The bromo-precursors were incompatible with the reaction conditions, under which they would undergo facile ring-opening side reactions. In addition to obtaining **16a–e** from the corresponding electron-rich iodobenzenes, it was found that heteroaromatic iodides could be coupled effectively to yield **16f–l** and **17a**. Included in the latter studies were substrates wherein the iodide was present on the carbon atoms of 3-thiophene, 5-benzofuran, 6- and 7-quinoline, as well as 3-, 5-, 6- and 7-indoles. A slight modification in the reaction conditions enabled the incorporation of vinyl and dienyl groups into the cyclotrypatamine scaffolds, as confirmed by the preparation of **16m–q** and **17b**. Note that vinyl bromides were used in excess because they were more prone to dimerization as compared with aryl iodides.[10a] Similar to our previous observation that electron-deficient aryl halides generally require DMAP as the ligand,[13] DMAP was necessary for the conversion into **17b** of the styrenyl bromide that contains an electron-withdrawing ester group.

As a further extension of the present method, chlorocyclotryptamines derived from *L*-tryptophan encompassing both the endo and exo-esters were subjected to the coupling conditions. Whereas the exo-ester precursor was highly effective for the coupling with *para*- methoxybenzene (giving **18**), the reaction with 7-iodoindole only furnished product **19** in 40% yield when DMF was used as solvent and the catalyst loading was increased to 20 mol%. In this case, the majority of the chloro substrate was converted into its *L*-tryptophan precursor via a dechlorination/decyclization process. The addition of a trace amount of water appears to be essential for the preparation of **18**, which possibly helps remove salts on Zn surface. By comparison, the endo-ester analog was more effective; it provided **20** in 60% yield. Since **20** can be viewed as the key scaffold of the natural product (+)-asperazine and (+)-pestalazine, the coupling of 7-iodotrptophan was pursued. This gave products **21** and **22** in 30% and 52% yields, respectively. Arylation of a C3-chloro tetracycle derived from Trp-Phe dipeptide with 7-iodotrptophan generated **23** in 13% yield. The major side reaction arose from dechlorination/decyclization of the chloro substrate to yield an indolic diketopiperazine. However, its assembly with 6-indolyl and 3,4,5-trimethoxyphenyl groups successfully furnished **24** and **25** in synthetically useful yields. It is worth noting that the joining of 7-indolyl derivatives with tertiary (Csp^3)–carbons is a recognized challenge as evidenced by Movassaghi's synthesis of asperazine and relevant analogs.[2b,17] The Friedel–Crafts methods employed by the authors may encounter a regioselective issue; only a 6% yield was observed for the key intermediate **23**.[2b] Finally, according to

Overman's studies, **22** should serve as a strong candidate for the construction of (+)-asperazine and its analogs.[14] Thus, saponification of **22** followed by assembly with *L*-phenylalanine provided **26**, which can be readily cyclized to form (+)-asperazine.[14]

Scheme 2. Formal Synthesis of (+)-Asperazine

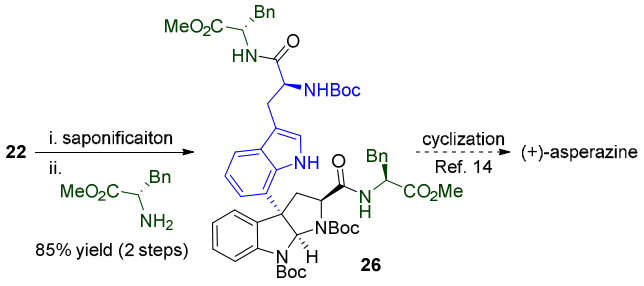

2.2. Mechanistic Investigations

We have carried out mechanistic studies on the present quaternary carbon-forming method, using a combination of experiments and DFT calculations.

2.2.1. Possible Reaction Pathways

Two pathways were considered, as shown in Scheme 3. The reaction may occur by a radical chain mechanism,[21] wherein oxidative addition of aryl halide to L_nNi^0 leads to $(L_n)Ni^{II}Ar(X)$ that intercepts *t*-Bu radical to give $(L_n)Ni^{III}Ar(t\text{-Bu})X$. Reductive elimination results in the *t*-Bu–Ar product and $(L_n)Ni^{I}X$. The latter abstracts bromide from *t*-BuBr and furnishes $(L_n)Ni^{II}X(Br)$ and *t*-Bu radical. While the radical diffuses to the bulk solution and combines with$(L_n)Ni^{II}Ar(X)$, $(L_n)Ni^{II}X(Br)$ is reduced to $(L_n)Ni^0$ by Zn, allowing the catalytic cycle to continue. An alternative double oxidative addition mechanism may also operate, which involves reduction of $(L_n)Ni^{II}Ar(X)$ to $(L_n)Ni^{I}Ar$ by Zn. The Ni(I) species abstracts bromide from *t*-BuBr, thereby generating *t*-Bu radical and $(L_n)Ni^{II}(Ar)Br$, which combine rapidly to give $(L_n)Ni^{III}(Ar)(t\text{-Bu})(Br)$.[25] Subsequent reductive elimination generates the product and $(L_n)Ni^{I}Br$ which is converted into $(L_n)Ni^0$ by Zn reduction.

Scheme 3. Proposed radical chain (left cycle) and double oxidative addition (right cycle) mechanisms

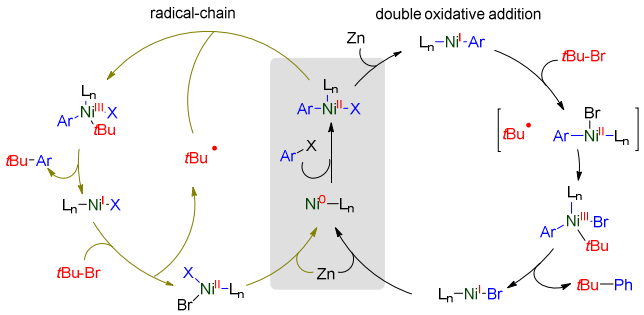

2.2.2. Involvement of Radicals

Under the standard reaction conditions, a bromotetrafuran tethered with allyl ether **27-H** was effectively coupled with 4-iodoanisole giving **28-H** in 50% yield. However, the germinal methyl peaks of **28-H** coincided as one singlet in the ^{1}H NMR spectrum.[16] Coupling of the deuterated analog **27-D** with methyl 4-bromobenzoate under the previously reported protocol for electron-withdrawing groups produced **29-D** with a syn/anti ratio of 1:1 (eq 1).[13] These results suggest that an alkyl radical was involved in the coupling process.[18]

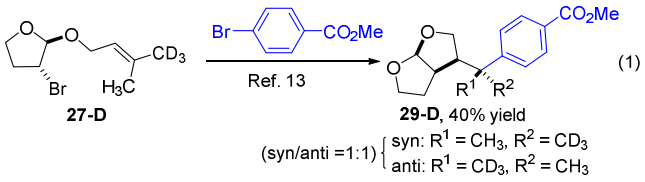

2.2.3. Preparation of $(Py)_nNiAr$ Complex

The use of pyridine or its derivatives is crucial for this quaternary carbon-forming process. To gain insight into the catalytically active species, we treated $Ni(COD)_2$ with methyl 4-bromobenzoate in the presence of excess DMAP in THF. A yellow precipitate was isolated and identified as a diamagnetic $[(DMAP)_3NiAr]^+Br^-$ complex (**30-Br**).[16,19-21] It should be noted that in solution, formation of a mixture containing low-coordinate pyridine-Ni complexes is also possible.[20b]

Exposure of **30-Br** to excess tertiary butyl bromide gave the quaternary product **31** in 40% yield (eq 2). This result was consistent with Weix's observation of a radical chain mechanism for the arylation of secondary alkyl halides with aryl halides.[22]

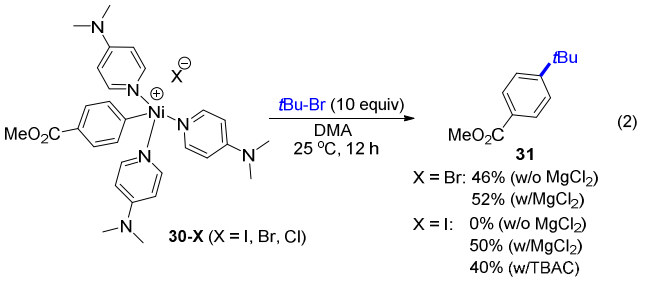

2.2.4 Effects of Salts

Treatment of $[(DMAP)_3Ni^{II}Ar]^+X^-$ (**30-X**; X = I, Br, Cl) with excess $MgCl_2$, LiCl, or $(n\text{Bu})_4NCl$ (TBAC) revealed complete conversion into a possible $(DMAP)_2Ni^{II}(Cl)Ar$ (**32**) species within 10 min, as confirmed by ^{1}H NMR studies (eq 3).[16,23] In eq 2, it was revealed that the reaction of **30-I** with *t*-BuBr did not give the quaternary product **31** unless $MgCl_2$ or $(n\text{Bu})_4NCl$ was added. These results suggest that complex **32** is most likely the intermediate intercepting the *t*-Bu radical and introducing reductive elimination of the product, wherein Mg^{2+} and Li^+ do not participate. By monitoring the reaction of **30-Br** with *t*-BuBr, we observed significant rate acceleration in the presence of $MgCl_2$ or TBAC (Figure S8), suggesting that formation of **32** is important for speeding up the reaction.

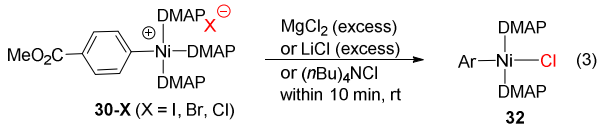

The important roles of $MgCl_2$ and LiCl in the catalytic process were further identified as follows.[16] First, the control experiments indicated that Mg^{2+}/Cl^- or Li^+/Cl^- ion pairs cooperatively determine the catalytic transformation efficiency (Table S2).[16] Without $MgCl_2$ and LiCl, with $(n\text{Bu})_4\text{NCl}$, or with $Mg(OTf)_2$ and LiOTf, no coupling reaction occurred (Table S2).[16] Second, both $MgCl_2$ and LiCl were able to activate Zn. Treatment of the mixture of tertiary alkyl bromide (**1**) and 4-iodoanisole with Zn/3-F-Py in DMA only resulted in recovered halides after 2 h. However, addition of $MgCl_2$ (1 equiv) or LiCl (3 equiv) resulted in substantial amounts of hydrodebromination and alkene products derived from **1** in both cases (Table S3).[16] Since Li^+/Cl^- ions are known to cooperatively solubilize the organozinc reagents formed on the surface of Zn,[24] the two salts in the present study may well function in a similar way by activating Zn. Third, $MgCl_2$ was found to react with a $Ni(acac)_2$/DMAP mixture and the pre-formed $(DMAP)_2Ni(acac)_2$ complex in DMSO-d_6 to afford more soluble Ni species, as confirmed by ^{1}H NMR studies. By contrast, LiCl was much less effective and $(n\text{Bu})_4\text{NCl}$ did not lead to detectable Ni complex signals at all (Tables S3–S4 and Figures S9–S12). This was attributed to stronger interaction of Mg^{2+} with acac anion.[16] Finally, reduction of the insoluble $(DMAP)_2$ $Ni(acac)_2$ complex in DMSO-d_6 to Ni(0) by Zn was not successful unless $MgCl_2$ was added (Table S5).[16]

2.2.5. *DFT Computational Study*

In view of the experimental findings above, we have employed DFT calculations in a bid to elucidate the two possible mechanisms shown in Scheme 3, using Ni^0Py_2 as the catalyst (**1cat**) and iodobenzene and *t*-BuBr as the substrates. Note that the formation of $(Py)_2Ni^0$ is more favorable than that of $(Py)_3Ni^0$ or $(Py)_4Ni^0$ (Figure S19). Oxidative addition of iodobenzene to $(Py)_2Ni^0$proceeds via the concerted transition state **TS1** to form the square planar Ni(II) complex **IM2** (Figure 4). This step has a readily attainable free energy of activation (7.8 kcal/mol) and large thermodynamic driving force (44.2 kcal/mol). **IM2** further coordinates with excess pyridine in the system to give **IM3**. The Ni–I bond distance in **IM3** suggests that it should be an ion pair with the iodide outside the coordination sphere. **IM3** dissociates to the cation **IM4** which

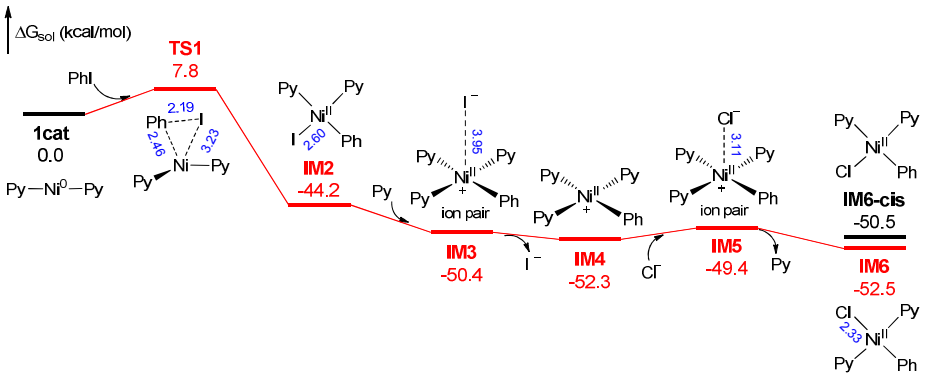

Figure 4. Free energy profile for the oxidative addition of PhI to $(Py)_2Ni^0$ and subsequent reactions. Selected bond distances are given in Å (the same below).

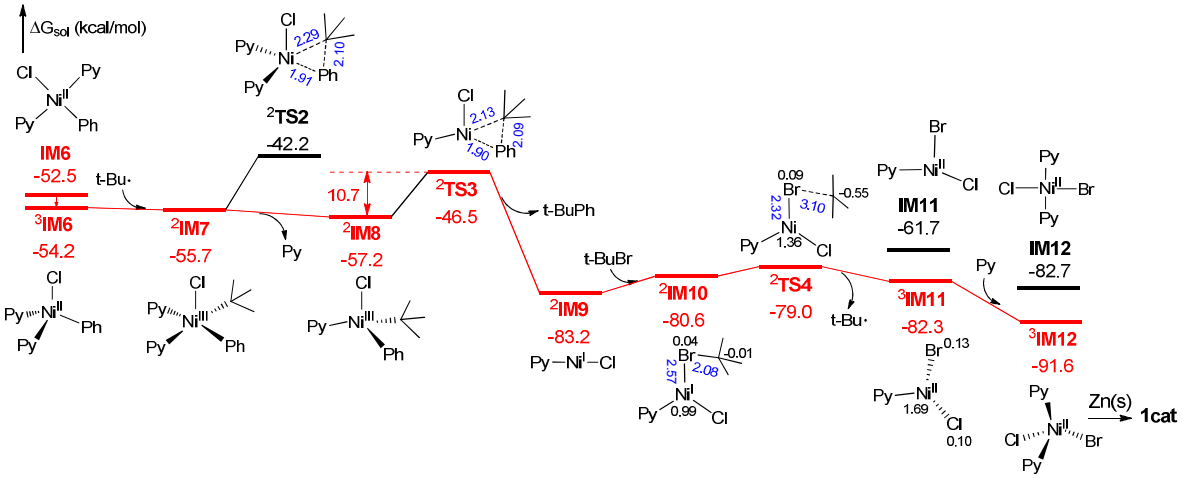

Figure 5. Free energy profile for the radical chain pathway with a Ni^{II}–Ni^{III} redox manifold following the oxidative addition. Upper left superscripts indicate the spin states of open-shell, paramagnetic structures (the same below). The numbers shown in black fonts on selected atoms in ^{2}**IM10**, ^{2}**TS4**, and ^{3}**IM11** denote spin densities.

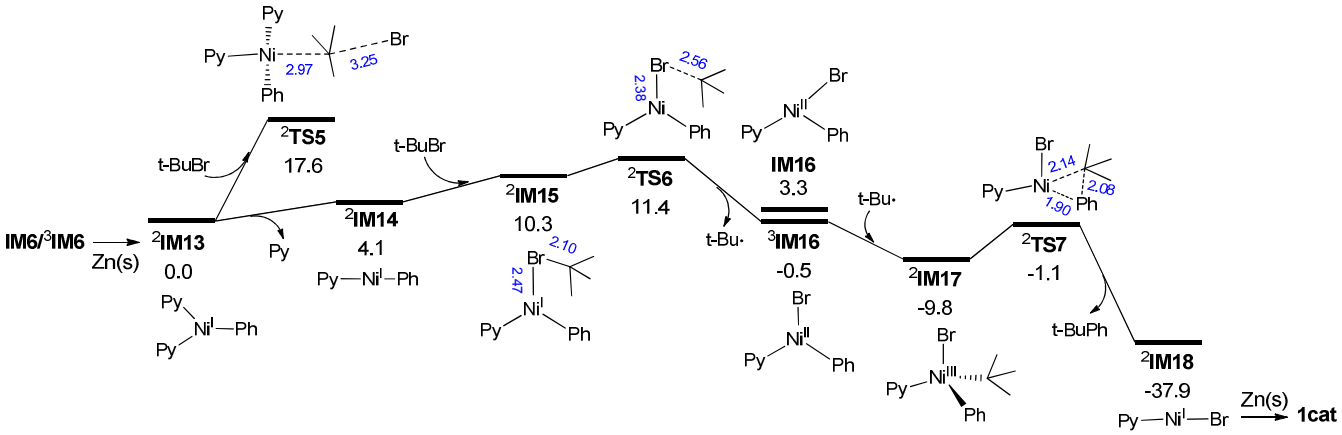

Figure 6. Free energy profile for the double oxidative addition pathway with a Ni^{I}–Ni^{II}–Ni^{III} redox manifold.

combines with chloride ion from the salt additives to form another ion pair, **IM5**.This ion exchange sets the stage for the ensuing substitution of chloride for pyridine, which would yield the trans complex **IM6** as the most stable intermediate in this phase of reaction. It is important to note that **IM3**/**IM4** and **IM6** correspond to the NMR-observed diamagnetic species described above as **30-X** and **32**. Thus, the calculations show good experimental–theoretical synergy.

We considered that **IM6** could convert to the tetrahedral triplet[26] ^{3}**IM6** by a Berry pseudorotation-type mechanism to facilitate the uptake of *t*-Bu radical by single electron transfer (SET) (Figure 5). ^{3}**IM6** has two unpaired electrons on the Ni(II) center, so it could readily utilize one of them to bond with the *t*-Bu radical to form the Ni(III) complex ^{2}**IM7**. Reductive elimination of *t*-BuPh from ^{2}**IM7** would meet the barrier ^{2}**TS2** that is 13.5 kcal/mol relative to ^{2}**IM7**. The alternative and more favorable pathway is by the dissociation of one pyridine ligand from ^{2}**IM7** to form ^{2}**IM8**, which then passes through the lower barrier ^{2}**TS3** ($\Delta G^{\neq}$ = 10.7 kcal/mol) to release the coupling product *t*-BuPh and generate the linear Ni(I) complex ^{2}**IM9**. Reductive elimination via three-coordinate ^{2}**IM8** and ^{2}**TS3** is more favorable than that through four-coordinate ^{2}**IM7** and ^{2}**TS2** because of steric effects. Reduced steric hindrance with decreasing coordination number stabilizes ^{2}**TS3** relative to ^{2}**TS2** more than it does ^{2}**IM8** relative to ^{2}**IM7** (^{2}**TS2** – ^{2}**TS3** = 4.3 kcal/mol, ^{2}**IM7** – ^{2}**IM8** = 1.5 kcal/mol). This is apparently because the transition states, wherein the *t*-Bu and aryl groups need to move closer, are more sensitive to changes in steric hindrance than are their precursor complexes.

Complex ^{2}**IM9** binds *t*-BuBr through the bromine donor atom to form ^{2}**IM10**, which then undergoes a facile intramolecular nickel-to-bromine SET via ^{2}**TS4** ($\Delta G^{\neq}$ = 4.2 kcal/mol relative to ^{2}**IM9**). This SET step leads to the triplet complex ^{3}**IM11** and regenerates the *t*-Bu radical, which is supported by spin analysis. As shown in Figure 5, the spin densities on the selected atoms in ^{2}**TS4** suggest that ^{2}**TS4** contains an emerging *t*-Bu radical with a spin density of 0.55 on the tertiary carbon, as well as an emerging triplet Ni(II) complex with a spin density of 1.36 on

the nickel center. The two spins apparently are antiferromagnetically coupled, making a net doublet of ^{2}**TS4**. ^{3}**IM11** combines with excess pyridine to form the more stable four-coordinate tetrahedral complex ^{3}**IM12**, which is then reduced by zinc to regenerate the catalyst $(Py)_2Ni^0$ (**1cat**). We can rule out the singlets of **IM11** and **IM12** on the basis of their much higher energies (Figure 5).

It should be noted that our computational results constitute a complex yet well-defined redox manifold throughout the reaction pathway from **1cat** to ^{3}**IM12**: $Ni^0 \rightarrow Ni^{II} \rightarrow Ni^{III} \rightarrow Ni^{I} \rightarrow Ni^{II}$. This is consistent with the fact that nickel as a 3d metal tends to engage in both one- and two-electron redox processes. Furthermore, in the complete reaction pathway, the reductive elimination via ^{2}**TS3** has the largest $\Delta G^{\neq}$ (10.7 kcal/mol) and is also irreversible, and as such, it is the rate-limiting step for the part of the reaction that takes place in solution. This readily attainable activation energy, coupled with the enormous overall thermodynamic driving force (–91.6 kcal/mol), explains the high activity of the catalyst system. We also investigated the electronic effects of the pyridine-type ligands on the activation energies of the reductive elimination (Figure S21).

Alternatively, the double oxidative addition mechanism suggests that aryl–Ni^I complexes could involve in the coupling with alkyl halides (Scheme 3). Thus, we considered the possible reduction of the Ni(II) complex **IM6** or ^{3}**IM6** by zinc to form Ni(I) complexes, which might furnish redox cycles different than what has been described above. Along these lines of thought, we computed the $(Py)Ni^IPh$ complexes ^{2}**IM13** and ^{2}**IM14** (Figure 6). For their oxidative addition reactions with *t*-BuBr, only the S_N2-type ^{2}**TS5** was located, and no concerted transition states were found. The pathway via ^{2}**TS5** is disfavored because it would require a much higher activation energy than the pathway via ^{2}**TS3** (Figure 5). ^{2}**IM14** could undertake an SET reaction with *t*-BuBr, similar to the SET reaction involving ^{2}**IM9**, which proceeds through ^{2}**IM15**, peaks at ^{2}**TS6**, and produces the Ni(II) complex ^{3}**IM16**. ^{3}**IM16** continues on another SET reaction with the *t*-Bu radical to form the Ni(III) complex ^{2}**IM17** with the alkyl ligand, which undergoes reductive elimination to give the coupling product *t*-BuPh and revert to the Ni^I oxidation state in ^{2}**IM18**. ^{2}**IM18** is then reduced by Zn to regenerate **1cat**. This double oxidative addition pathway would contain a $Ni^I \rightarrow Ni^{II} \rightarrow Ni^{III}$ manifold and have the rate-limiting barrier ^{2}**TS6** ($\Delta G^{\neq}$ = 11.4 kcal/mol relative to ^{2}**IM13**). ^{2}**TS6** is relatively 0.7 kcal/mol (11.4 – 10.7) higher than ^{2}**TS3**, the rate-limiting barrier in the radical chain pathway (Figure 5), but because this energy gap is rather small, we cannot rule out either mechanism.

3. CONCLUSIONS

In summary, we have shown that 3-F-pyridine, in conjunction with Ni(II) salts in the presence of $MgCl_2$, LiCl and Zn allows the coupling of electron-rich aryl iodides with tertiary alkyl halides. This coupling method is attractive in that it affords an efficient means of creating quaternary carbon centers. The mild Ni-catalyzed reductive conditions associated with this procedure accommodate a wide variety of functional groups, thereby allowing a broad substrate scope. The compatibility of heteroaromatic iodides, particularly 7-iodoindoles, may provide facile access to a number of structurally-relevant naturally-occurring products whose preparation could otherwise prove challenging using conventional coupling methods. The DFT computations give the free energy profiles of two possible reaction coordinates: the radical chain and the double oxidative addition pathways. The choice of the pyridine ligand appears to be pivotal in that it plays a crucial role in controlling the dissociation and recombination of various Ni-containing intermediates. $(Py)_2Ni$ complexes are key for oxidative addition of aryl halides to Ni^0, whereas $(Py)_2Ni(Ar)Cl$ complexes are key for radical interception. Although the DFT computations have given mechanistic insights into the part of the reaction that takes place in solution, the overall rate and time of this coupling reaction could be governed by the heterogeneous process that generates the active catalyst.[27] We believe that the present study is not only of operational interest in terms of forming otherwise challenging-to-prepare C–C bonds, but it also provides mechanistic insights for other relevant nickel-mediated coupling reactions.

ASSOCIATED CONTENT

Supporting Information. Methods, experimental procedures, characterizations of new compounds, and additional computational results. This material is available free of charge via the Internet at http://pubs.acs.org.

AUTHOR INFORMATION

Corresponding Authors

hegui_gong@shu.edu.cn, xiaotai.wang@ucdenver.edu

Author Contributions

‖ These authors contributed equally.

ACKNOWLEDGMENT

We acknowledge support for this work by the NSF of China (Nos. 21572140 and 21372151), the One Hundred-Talent Program of Shanxi Province, and the University of Colorado Denver. We thank Jiawang Wang and Changzhou Cheng for purifying the compounds in Figure 3, and Dr. Xiaolong Wan (SIOC, China) for purifying compound **32**. We thank Prof. Jonathan Sessler (Univ. of Texas) for manuscript proofreading. We also thank Profs. Tom Cundari (North Texas Univ.), Michael Hall (Texas A&M Univ.), Keith Woo (Iowa State Univ.), and Yanfeng Dang (Tianjin Univ.) and Mr. Xi Deng for helpful discussions.

REFERENCES

(1) Selected reviews: (a) Zi, W.; Zuo, Z.; Ma, D. *Acc. Chem. Res.* **2015**, *48*, 702. (b) Kim, J.; Movassagh, M. *Acc. Chem. Res.* **2015**, *48*, 1159–1171. (c) Chen, W.; Zhang, H. *Sci. China Chem.* **2016** *59*, 1065. (d) Liu, Y.; Han, S.-J.; Liu, W.-B.; Stoltz, B. M. *Acc. Chem. Res.* **2015**, *48*, 740. (e) Rui-Sanchis, P.; Savina, S. A.; Albericio, F.; Alvarez, M. *Chem.–Eur. J.* **2011**, *17*, 1388.

(2) (a) Kim, J.; Movassaghi, M. *J. Am. Chem. Soc*. **2011**, *133*, 14940. (b) Loach, R. P.; Fenton, O. S.; Movassaghi, M. *J. Am. Chem. Soc*. **2016**, *138*, 1057. (c) Nicolaou, K. C.; Liu, G.; Beabout, K.; McCurry, M. D.; Shamoo, Y. *J. Am. Chem. Soc*. **2017**, *139*, 3736. (c) Spittler, M.; Lutsenko, K.; Czekelius, C. *J. Org. Chem*. **2016**, *81*, 6100.

(3) Coupling of *tertiary* R-MgX catalyzed by Ni: (a) Lohre, C.; Dröge, T.; Wang, C.; Glorius, F. *Chem.–Eur. J.* **2011,** *17*, 6052. (b) Joshi-Pangu, A.; Wang, C.–Y.; Biscoe, M. R. *J. Am. Chem. Soc.* **2011**, *133*, 8478.

(4) Cu- and Co-catalyzed coupling of *tertiary* R-MgX with alkyl halides: (a) Terao, J.; Todo, H.; Begum, S. A.; Kuniyasu, H.; Kambe, N. *Angew. Chem., Int. Ed.* **2007**, *46*, 2086. (b) Ren, P.; Stern, L. A.; Hu, X. L. *Angew. Chem., Int. Ed*. **2012**, *51*, 9110. (c) Yang, C.–T.; Zhang, Z.–Q.; Liang, J.; Liu, J.–H.; Lu, X.–Y.; Chen, H.–H.; Liu, L. *J. Am. Chem. Soc.* **2012**, *134*, 11124. (d) Iwasaki, T.; Takagawa, H.; Singh, S. P.; Kuniyasu, H.; Kambe, N. *J. Am. Chem. Soc.* **2013**, *135*, 9604.

(5) Primer, D. N.; Molander, G. A. *J. Am. Chem. Soc.* **2017**, *139*, 9847.

(6) Zultanski, S. L.; Fu, G. C. *J. Am. Chem. Soc*. **2013**, *135*, 624.

(7) Coupling of Ar–MgX with admantanyl chloride: (a) Ghorai, S. K.; Jin, M.; Hatakeyama, T.; Nakamura, M. *Org. Lett*. **2012**, *14*, 1066. (b) Direct coupling of Ar_2Zn with *t*Bu–Br and admantanyl–Br: Dunsford, J. J.; Clark, E. R.; Ingleson, M. J. *Angew. Chem., Int. Ed.* **2015**, *54*, 5688. Coupling of styrenyl aziridines with organozincs to give all quaternary carbon products: (c) Huang, C.-Y.; Doyle, A. G. *J. Am. Chem. Soc*. **2015**, *137*, 5638.

(8) For recent reviews on reductive coupling of two electrophiles, see: (a) Knappke, C. E. I.; Grupe, S.; Gärtner, D.; Corpet, M.; Gosmini, C.; von Wangelin, A. J. *Chem. –Eur. J*. **2014**, *20*, 6828. (b) Everson, D. A.; Weix, D. J. *J. Org. Chem***. 2014**, *79*, 4793. (c) Moragas, T.; Correa, A.; Martin, R. *Chem. –Eur. J*. **2014**, *20*, 8242. (d) Wang, X.; Dai, Y.; Gong, H *Top. Curr. Chem. (Z)* **2016**, *374*, 43.

(9) Acylation of admantanyl chloride with CO_2 and of unactivated tertiary alkyl halides with acid anhydrides: (a) Börjesson, M.; Moragas, T.; Martin, R. *J. Am. Chem. Soc*. **2016**, *138*, 7504. (b) Zhao, C.; Jia, X.; Wang, X.; Xue, W. *J. Am. Chem. Soc*. **2014**, *137*, 17645.

(10) Reductive allylation of tertiary alkyl halides with allylic carbonates and acetates: (a) Chen, H.; Jia, X.; Yu, Y.; Qian, Q. Gong, H. *Angew. Chem., Int. Ed*. **2017**, *56*, 13103-13106. (b) Gosmini C. *Angew. Chem., Int. Ed*. **2011**, *50*, 10402.

(11) Dimerization of activated *tertiary* alkyl halides: (a) Peng, Y.; Luo, L.; Yan, C.–S.; Zhang, J.–J.; Wang, Y.–W. *J. Org. Chem.* **2013**, *78*, 10960. (b)Wada, M.; Murata, T.; Oikawa, H.; Oguri, H. *Org. Biomol. Chem.* **2014**, *12*, 298.

(12) Selected examples of arylation of primary and secondary alkyl halides using cross-electrophile coupling methods: (a) Cherney, A. H.; Kadunce, N. T.; Reisman, S. E. *J. Am. Chem. Soc.* **2013**, *135*, 7442. (b) Everson, D. A.; Jones, B. A.; Weix, D. J. *J. Am. Chem. Soc.* **2012,** *134*, 6146–6159. (c) Zhao, Y.; Weix, D. J. *J. Am. Chem. Soc.* **2014**, *136,* 48. (d) Tellis, J. C.; Primer, D. N.; Molander, G. A. *Science* **2014**, *345*, 433. (e) Zuo, Z.; Ahneman, D, T.; Chu, L.; Terrett, J. A.; Doyle, A. G.; MacMillan, D. W. C. *Science* **2014**, *345*, 437.

(13) Wang, X.; Wang, S.; Xue, W.; Gong, H. *J. Am. Chem. Soc.* **2015**, *137*, 11562.

(14) The seminal work reported by Overman et al. required over 20 steps of reaction to synthesize the intermediate **26** starting from (*R*)-serine. References: (a) Goverk, S. P.; Overman, L. E. *J. Am. Chem. Soc.* **2001**, 123, 9469. (b) Govek, G. P.; Overman, L. E. *Tetrahedron Lett*. **2007**, *63*, 8499.

(15) The reaction conditions were described in Ref. 13, which involved $Ni(acac)_2$ (10%), DMAP (30%), and $MgCl_2$ (150%).

(16) See the Supporting Information (SI) for details.

(17) For additional natural products containing C8'-indole derivatives such as (-)-hodgkinsine, (-)-calycosidine, (-)-quadrigemine I, (-)-quadrigemine C and (-)-psycholeine, see: Lindovska, P.; Movassaghi, M. *J. Am. Chem. Soc.* **2017**, *139*, 17590.

(18) Creutz, S. E.; Lotito, K. J.; Fu, G. C.; Peters, J. C. *Science* **2012**, *338*, 647.

(19) Although an X-ray single crystal structure of **30-Br** was not available, its formation was confirmed by ^{1}H and ^{13}C NMR coupled with high resolution mass spectrometry (see the Supporting Information for details).

(20) References on bis- and tris(pyridine)–Ni complexes: (a) Cámpora, J.; del Mar Conejo, M.; Mereiter, K.; Palma, P.; Pérez C.; Manuel L. Reyes, M. L.; Ruiz, C. *J. Orgmetall. Chem.* **2003**, *683*, 220. (b) Feth, M. P.; Klein, A. Helmut Bertagnolli, H. *Eur. J. Inorg. Chem***. 2003**, 839.

(21) Diamagnetic ^{1}H NMR for complexes **30-X** (X = Cl, Br, I) was observed in DMSO-d_6, supporting the square planar Ni(II) coordination geometry. The ionic nature of **30-X** was further verified by conductivity measurement in DMA.

(22) (a) Biswas, S.; Weix, D. J. *J. Am. Chem. Soc.* **2013**, *135*, 16192. See also: (b) Schley, N. D.; Fu, G. C. *J. Am. Chem. Soc*. **2014**, *136*, 16588. (c) Gutierrez, O.; Tellis, J. C.; Primer, D. N.; Molander, G. A.; Kozlowski, M. C. *J. Am. Chem. Soc*. **2015**, *137*, 4896.

(23) For [(bpy)Ni(Mes)I], a known compound, the iodide dissociation rate was found to be fast (k = 0.176 $M^{-1}S^{-1}$), but its chloride analog undergoes extremely slow dissociation ($k = 5.18 \times 10^{-5}$ $M^{-1}S^{-1}$). Therefore, formation of the more stable Ni–Cl bond in complex **32** is plausible. References on [(bpy)Ni(Mes)I]: (a) Klein, A.; Kaiser, A.; Wielandt, W.; Belaj, F.; Wendel, E.; Bertagnolli, H.; Záliš, S. *Inorg. Chem.* **2008**, *47*, 11324. (b) Hamacher, C.; Hurkes, N.; Kaiser, A.; Klein, A. *Z. Anorg. Allg. Chem.* **2007**, 633, 2711.

(24) Feng, C.; Cunningham, D. W.; Easter, Q. T.; Blum S. A. *J. Am. Chem. Soc.* **2016**, *138*, 11156.

(25) Jones, G. D.; Martin, J. L.; McFarland, C.; Allen, O. R.; Hall, R. E.; Haley, A. D.; Brandon, R. J.; Konovalova, T.; Desrochers, P. J.; Pulay, P.; Vicic, D. A. *J. Am. Chem. Soc.* **2006**, *128*, 13175.

(26) Vitek, A. K.; Leone, A. K.; McNeil, A. J.; Zimmerman, P. M. *ACS Catal.* **2018**, *8*, 3655.

(27) In an analogous study by Weix (ref 12b), the overall rate for the coupling of a primary alkyl bromide with bromobenze was found to be controlled by activation of Zn. Given the heterogeneous nature of the present catalytic process, the reaction rate can be affected by various factors, including the complex functions of the Ni precatalyst, $MgCl_2$/LiCl additives, and Zn reductant (see the section of Mechanistic Investigations in the Supporting Information for details).

TOC

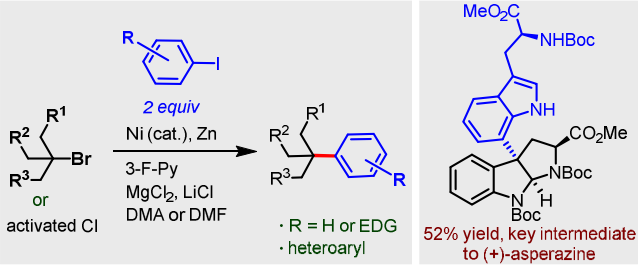
R
I
2 equiv
Ni (cat.), Zn
3-F-Py
MgCl2, LiCl
DMA or DMF
R1
R2
R3
Br
or
activated Cl
· R = H or EDG
· heteroaryl
MeO2C
NHBoc
NH
CO2Me
NBoc
N
H
Boc
52% yield, key intermediate
to (+)-asperazine